ACS OMEGA

http://pubs.acs.org/journal/acsodf

Article

Exclusion of Anchor-Matched Peptide Nucleic Acid from Liquid-Ordered Domains by Hybridization with Complementary Flavin-Labeled DNA

Yoshimi Oka*

Cite This: *ACS Omega* 2023, 8, 1109−1113

Read Online

ACCESS | Metrics & More | Article Recommendations | Supporting Information

ABSTRACT: Membrane-anchored proteins and their mimics, such as peptide nucleic acids (PNAs), are known to partition preferentially into either lipid raft/liquid-ordered (lo) domains or into non-raft/liquid-disordered (ld) domains, depending on their lipophilic anchors. Here, anchor-matched PNA was demonstrated to be excluded from the lo microdomains of giant unilamellar vesicles by hybridization with the complementary flavin-labeled DNA. As shown in control experiments using Alexa Fluor 488-labeled DNA, which showed that the preferential partitioning was the lo domain, the domain distribution of PNA was not only dependent on the lipophilic anchor but also on the structure of the hybridized DNA or PNA pair. In such systems, the main factors that influence changes in the domain selectivity of the probes are most likely to also be interactivity (i.e., steric bulkiness), hydrophilicity, and self-assembling ability. These findings may have the potential to contribute to the elucidation of membrane-active peptides, the method of their activation, and their applications in medicine such as antimicrobial use, especially with regard to their actions at the interface between the lo and ld domains in cells.

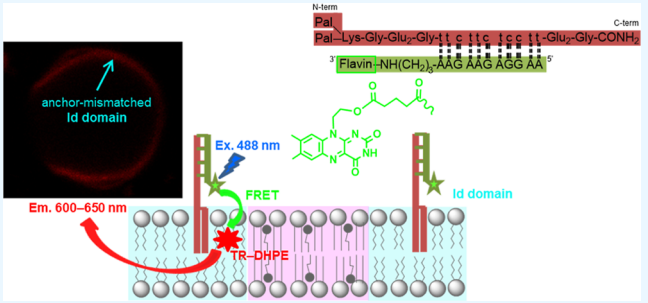

1. INTRODUCTION

Microdomain structures (lipid rafts) formed in cell membranes are known to function as platforms for the specific recruitment of proteins related to transport and signal transduction.[1,2] Many studies have been conducted on model membrane systems that consist of liquid-ordered (lo) and liquid-disordered (ld) domains, the former of which is formed predominantly by saturated lipid and cholesterol (Chol), whereas the latter of which is formed predominantly by unsaturated lipid through phase separation, as well as the cell membrane.[3−6] The development of fluorescent probes and the use of confocal microscopy have recently made it possible to visualize micrometer-sized lo and ld domains in giant unilamellar vesicles (GUVs).[7−12] Noteworthy lipophilic nucleic acid-based fluorescent probes have been reported that exploit the self-assembly properties of the complementary oligonucleotides to enable controlled targeting and immobilization of specific molecules and liposomes to membranes.[13−16] In such systems, the probes partition preferentially, either into lo or ld domains, depending on their lipophilic anchors. Membrane-anchored peptide nucleic acid (PNA) (in a defined sequence of **PNA_C16** in the literature: Pal-Lys(Pal)-Gly-Glu_2-Gly-ttc ttc tcc tt-Glu_2-Gly-$CONH_2$, in which Pal refers to a palmitoyl chain and multiple Glu sequences allow PNA to become more hydrophilic and to stabilize sticking out to the water phase, as shown in Scheme 1) that partitions exclusively into lo domains of model membranes and visualization by hybridization with a fluorescently labeled complementary DNA strand have been reported.[13,14] Furthermore, fluorophores such as Alexa and flavin have been reported to be quenched by some amino acids, such as Trp and Tyr,[17,18] which are preferable to avoid unless otherwise constrained or intended.[19−21] With reference to these reports, we have also demonstrated that **PNA_C16**/Alexa Fluor 488-labeled DNA (**AF488−DNA**)[21] and **PNA_C16**/flavin-labeled PNA (**Flavin−PNA**) hybrids[22] are distributed in lo domains of GUVs, although the latter hybrid displays disruption of the interfaces between the lo and ld domains after targeting the lo domain.

Here, the author has focused on a new flavin probe composed of **PNA_C16** and its complementary DNA labeled at the 3′-end with a flavin derivative synthesized in this study (Schemes 1 and 2). The results showed that this probe was distributed in the opposite domains of GUVs to those predicted by anchor-matched domains. This report describes the synthesis of the flavin derivative, preparation of GUVs using an electroformation method, observation of the domain distribution for the **PNA_C16/Flavin−DNA 2** hybrid, and fluorescence resonance energy transfer (FRET) detection using **Flavin−DNA 2** as a

Received: October 7, 2022
Accepted: December 2, 2022
Published: December 16, 2022

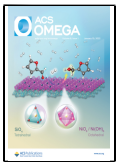

© 2022 The Author. Published by American Chemical Society

Scheme 1. Schematic Illustration of Palmitoylated PNA (PNA_C16) and Its Complementary DNA Labeled with Flavin (Flavin−DNA 2) Partitioned Into Ld Microdomains of GUVs

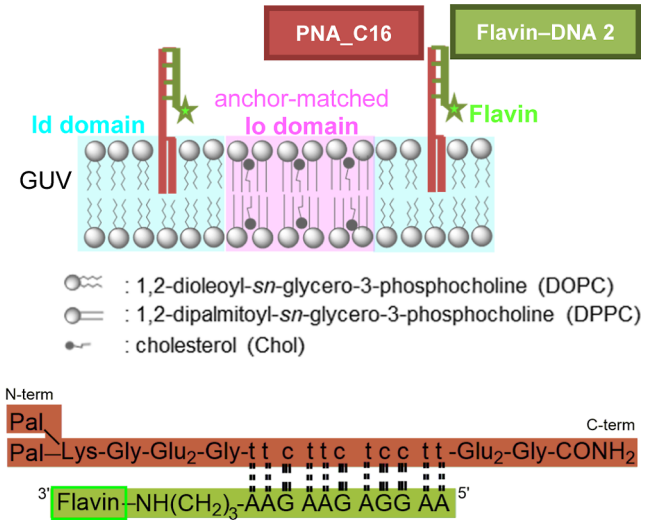

donor across a water−membrane interface. The findings suggest that the domain distribution of membrane-anchored PNA is not only dependent on the lipophilic anchor but also on the structure of the hybridized DNA or PNA pair, which may have the potential to contribute to the elucidation of membrane-active peptides and provide applications in medicine such as antimicrobial use,[23−30] especially in acting at an interface between lo and ld domains in cells.

2. RESULTS AND DISCUSSION

The flavin derivative was initially synthesized to obtain a DNA oligonucleotide labeled with flavin (Flavin−DNA). Similar to the previously reported **Flavin−PNA**,[21] labeling of DNA with 3-(7′,8′-dimethylisoalloxazin-10′-yl)propanoic acid (**Flavin−DNA 1**) was tested, and the results indicated that the **PNA_C16/Flavin−DNA 1** hybrid was not distributed in GUVs, probably due to the poor aqueous solubility of **Flavin−DNA 1**. Therefore, to improve the hydrophilicity of the flavin derivative, hydrophilic riboflavin and glutaric anhydride were used as starting materials for the synthesis. The synthesis of 5-(2-(7′,8′-dimethylisoalloxazin-10′-yl)-ethoxy)-5-oxopentanoic acid, that is, the labeling molecule for **Flavin−DNA 2**, is shown in Scheme 2.

The DOPC/DPPC/Chol GUV sample was observed using confocal fluorescence microscopy to assess whether the flavin probe, **PNA_C16/Flavin−DNA 2** hybrid, has domain selectivity. Figure 1 shows the confocal fluorescence image of

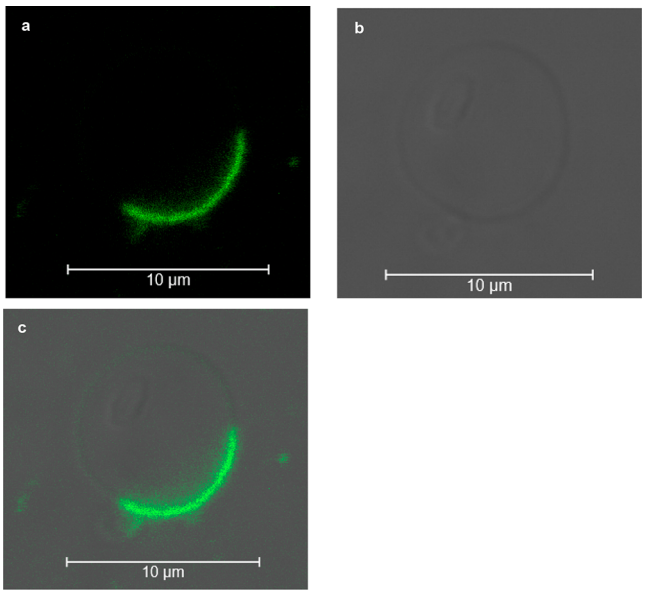

Figure 1. Confocal fluorescence image (a) and differential interface contrast image (b) of 1,2-dioleoyl-*sn*-glycero-3-phosphocholine (DOPC)/1,2-dipalmitoyl-*sn*-glycero-3-phosphocholine (DPPC)/Chol GUV with the incorporated **PNA_C16/Flavin−DNA 2** hybrid. (c) Merged image of (a) and (b). Excitation: 488 nm; detection: 500−550 nm.

GUV composed of the μm-scaled domain with the incorporated **PNA_C16/Flavin−DNA 2** hybrid. According to the green fluorescence of flavin, **PNA_C16/Flavin−DNA 2** hybrid almost exclusively partitions into one side of the microdomain. By quantitative analysis using emission intensity profiles (as shown in Figure S3), the fluorescence intensity of flavin partitioning into the domain with the incorporated hybrid was calculated to be 168 (16) (Figure 2), whereas the intensity on the opposite side of domain across the GUV center was calculated to be 21 (4). Therefore, the ratio of flavin fluorescence intensity in the probe-rich domain/probe-poor domain resulted to be 8.2, which is comparable to the ratio 7.6 for the lo/ld fluorescence intensity of AF488 in the **PNA_C16/AF488−DNA** hybrid partitioned into DOPC/DPPC/Chol GUV.[21]

In the next step, which domain incorporates the flavin probe (i.e., **PNA_C16/Flavin−DNA 2** hybrid) was examined by dual-probe fluorescence experiments using Texas Red−1,2-dipalmitoyl-*sn*-glycero-3-phosphoethanolamine (TR−DHPE). In the sequential scanning mode, flavin was excited with a 488 nm argon laser, and fluorescence was recorded at 500−550 nm, and then, TR-DHPE was excited with a 561 nm diode-pumped solid-state (DPSS) green laser, and fluorescence was recorded at 600−650 nm. Figure 3 shows confocal fluorescence images of

Scheme 2. Synthesis of 5-(2-(7′,8′-Dimethylisoalloxazin-10′-yl)ethoxy)-5-oxopentanoic Acid

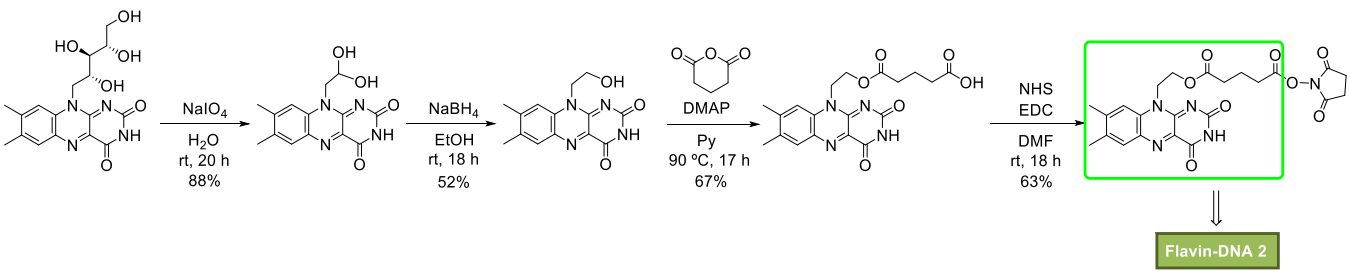

https://doi.org/10.1021/acsomega.2c06463
ACS Omega 2023, 8, 1109−1113

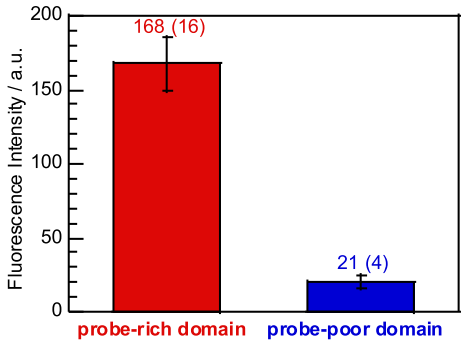

Figure 2. Fluorescence intensities of flavin in both of the GUV domains with the incorporated **PNA_C16/Flavin−DNA 2** probe under a microscope. For the respective domains, the averages and standard deviations of five points are plotted. The fluorescence emission profiles are shown in Figure S3.

the GUVs composed of micrometer-scaled domains with the incorporated **PNA_C16/Flavin−DNA 2** hybrid and TR-DHPE. Based on the red fluorescence image, TR−DHPE was almost exclusively partitioned into the ld domain (Figure 3b). The green fluorescence of flavin on the **PNA_C16/Flavin−DNA 2** hybrid was observed in the identical domain, that is, the ld domain (Figure 3a). FRET in dual-fluorophore-labeled domains of GUVs was also assessed. The flavin moiety in the **PNA_C16/Flavin−DNA 2** hybrid partitioned into the ld domain was excited by a 488 nm laser, and fluorescence could be detected not only at 500−550 nm (Figure 3a) but also at 600−650 nm (Figure 3d), the latter being due to FRET from the flavin to TR−DHPE. Consequently, the flavin on the **PNA_C16/Flavin−DNA 2** hybrid appears to protrude from

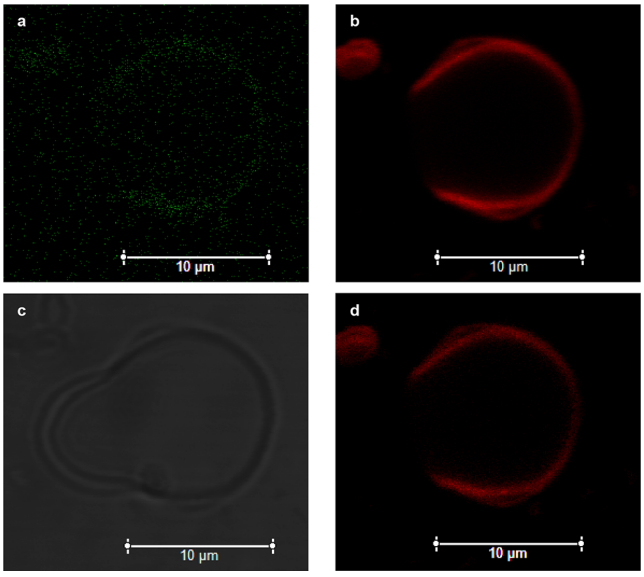

Figure 3. Confocal fluorescence and differential interface contrast images of DOPC/DPPC/Chol GUVs with the incorporated **PNA_C16/Flavin−DNA 2** hybrid and TR−DHPE. (a) Distribution in the ld domains determined from the green fluorescence of flavin was verified from (b) the identical ld domains labeled by TR−DHPE as red fluorescence. The domains remain stable according to the differential interference contrast image (c). (d) FRET image of ld domains in GUV with the incorporated **PNA_C16/Flavin−DNA 2** hybrid and TR−DHPE. Excitation: 488 nm; detection: (a) 500−550 nm and (d) 600−650 nm. (b) Excitation: 561 nm; detection: 600−650 nm.

Scheme 3. Schematic Illustration of FRET from the PNA_C16/Flavin−DNA 2 Hybrid to TR-DHPE Partitioned Into Ld Microdomains of GUVs

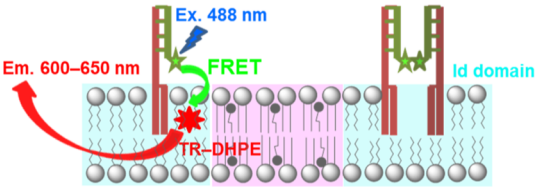

the ld domain toward the aqueous phase; the FRET to TR−DHPE in the ld domain occurs well across the water−ld domain interface, as illustrated in Scheme 3. The flavin fluorescence appears to diminish (Figure 3a) in accordance with efficient FRET (Figure 3d).

However, this result is inconsistent with the reported partitioning preference of the **PNA_C16**/DNA hybrids.[13,21] The partitioning into the lo domain of the **PNA_C16/AF488−DNA** hybrid[21] was again confirmed simultaneously under the same conditions as the **PNA_C16/Flavin−DNA 2** hybrid, as shown in Figure S4. These results indicate that the partitioning preference of **PNA_C16**, either into lo or ld domains, is strongly dependent on the labeling molecules of the complementary DNA, that is, flavin or AF488. This result raises the questions of whether a lipophilic anchor always allows its linking probe to be partitioned into matched domains. In this regard, we have previously demonstrated that the **PNA_C16/Flavin−PNA** hybrid targets the lo domains and disrupts their interface to ld domains and that the **PNA_C16/AF488−PNA** hybrid also acts as a similar membrane-active probe.[22] In that report, we concluded that the disruption through the vesiculations and probe aggregations, which were observed from time-lapse images, may be induced by the redistribution of the PNA duplex and formation of large curvatures at the lo−ld interfaces.[22] According to the literature, the lipid-anchored DNA system having hydrophobic fluorophores such as the dipalmitoyl anchor−chalcon fluorophore−DNA oligomer tends to form a self-assembled structure in an aqueous environment and not to partition into membranes.[31] In contrast, the lipid−hydrophilic (AF488) fluorophore−DNA oligomer has been reported to be distributed uniformly in both of the domains of DOPC/egg sphingomyelin/Chol GUVs, where it could be explained that the hydrophilic fluorophore permits the probe to partition into membranes and ether-linked glycerophospholipids used in the system are more loosely packed in membranes and thereby increase their fluidity.[32] These reports are consistent with the fact that the **PNA_C16/Flavin−DNA 1** hybrid was not distributed in GUVs due to hydrophobic flavin fluorophore, and with slightly higher hydrophilicity by the modification of glutaric anhydride, the **PNA_C16/Flavin−DNA 2** hybrid came to be distributed in GUVs. Considering the three cases in our study together, the dipalmitoyl anchors of **PNA_C16** are common and matched for the lo domain constituted by DPPC and Chol. In contrast, the binding interactions of PNA and DNA hybrids are most likely different from PNA duplexes, that is, the former has weaker binding than the latter, which results in the former being more sterically bulky, based on the reported thermal stabilities for these types of duplexes.[33] Another difference is the hydrophilicity of the complementary strands themselves and their labeling molecules, and the latter has a strong influence on the distribution in GUVs and partitioning preference into the domains, especially in the

https://doi.org/10.1021/acsomega.2c06463
ACS Omega 2023, 8, 1109−1113

case of PNA/DNA hybrids. The AF488 moiety should not inhibit the high aqueous stability of the DNA moiety in **AF488−DNA** due to the zwitterionic character at neutral pH. On the other hand, despite improvement in the hydrophilicity of the flavin derivative in this study, the flavin moiety may inhibit the aqueous stability of the DNA moiety and carry self-assembling properties in **Flavin−DNA 2**, which leads to **PNA_C16** being partitioned into the domains of higher fluidity, that is, ld domains, by hybridization. The results of this study may indicate the possibility of activating domain selectivity for a membrane-anchored mimic protein (e.g., **PNA_C16**) by changing the interactivity, hydrophilicity, and self-assembling ability of the interactor (e.g., **Flavin−DNA 2**). A possible manner of self-assembling **PNA_C16/Flavin−DNA 2** hybrid in the ld domain at present is also illustrated in Scheme 3. Further experiments using the dipalmitoyl anchor−multiple Glu peptide−fluorophore−DNA oligomer such as 5′-Pal-Lys(Pal)-Gly-Glu2-Gly-Flavin-TTC TTC TCC TT-3′ and its hybrid with PNA (i.e., aa gga gaa gaa) may be compared with the present results and provide more detailed explanation; however, such a type of flavin-tethered DNA is hard to synthesize by conventional methods[34,35] and requires the form with unmodified 3 and 5 positions (i.e., modified 7, 8, and/or 10 positions) of the isoalloxazine ring.

3. CONCLUSIONS

In conclusion, PNA with a dipalmitoyl anchor (**PNA_C16**) was excluded from the lo microdomains of DOPC/DPPC/Chol GUVs by hybridization with the complementary flavin-labeled DNA (**Flavin−DNA 2**), despite the lo domains being composed of DPPC as the main component. A new flavin derivative was synthesized from riboflavin and glutaric anhydride to improve the hydrophilicity of the flavin moiety and its resultant **Flavin−DNA 2**. The **PNA_C16/Flavin−DNA 2** hybrid was demonstrated to be preferentially partitioned into the ld microdomain with the selectivity ratio of ld/lo = 8.2 and to remain stable by single- and dual-fluorescence experiments. Furthermore, FRET from flavin on the **PNA_C16/Flavin−DNA 2** hybrid to TR−DHPE across the water−ld domain interface was demonstrated. Control experiments using **PNA_C16/AF488−DNA** (under the same conditions as the **PNA_C16/Flavin−DNA 2** hybrid) showed that the preferential partitioning was the lo domain; therefore, the domain distribution of membrane-anchored PNA was dependent not only on the lipophilic anchor but also on the structure of the hybridized DNA or PNA pair. The main factors that influence changes in the domain selectivity of the probes, except for the anchor structure, seem to be interactivity (i.e., steric bulkiness), hydrophilicity, and self-assembling ability. The results obtained here may have the potential to contribute to the elucidation of membrane-active peptides, their activation method, and their applications in medicine, especially with regard to their actions at the interface between the lo and ld domains in cells.

4. EXPERIMENTAL SECTION

GUVs were prepared from a mixture of DOPC, DPPC, and Chol in a 2:2:1 mole ratio using an electroformation method. The sample preparation protocol was the same as reported previously in refs 21 and.[22] TR−DHPE (0.05 mol %, relative to the lipid mixture), which is known to be a probe with a preference for the ld domain, was added to the lipid mixture. After the formation of GUVs, ca. 0.02 mol % (relative to the initial amount of lipid mixture) palmitoylated PNA and the complementary DNA labeled with flavin or AL488 were added to the vesicle suspension, which was then incubated at 25 °C for 1 d. The final ratio of GUV buffer/DMSO was adjusted to 10. All images were taken using a confocal microscope (Leica TCS-SP8 or Zeiss LSM 700) with a 63× (NA 1.2) oil immersion objective at room temperature (ca. 20 °C). Using the sequential scanning mode, flavin and AL488 were excited with a 488 nm argon laser, the fluorescence was recorded at 500−550 nm, and TR−DHPE was excited with a 561 nm DPSS Green laser and recorded at 600−650 nm, except for FRET observation. A resolution of 512 pixel × 512 pixel and a scan speed of 400 Hz were used.

■ ASSOCIATED CONTENT

Supporting Information

The Supporting Information is available free of charge at https://pubs.acs.org/doi/10.1021/acsomega.2c06463.

Experimental details of synthesis, confocal fluorescence images, and fluorescence emission profiles (PDF)

■ AUTHOR INFORMATION

Corresponding Author

Yoshimi Oka − *Research Promotion Institute, Oita University, Oita 870-1192, Japan;* Present Address: Hiroshima University, 1-3-1 Kagamiyama, Higashihiroshima 739-8526, Japan; orcid.org/0000-0002-4137-766X; Email: yoshimo@hiroshima-u.ac.jp

Complete contact information is available at: https://pubs.acs.org/10.1021/acsomega.2c06463

Notes

The author declares no competing financial interest.

■ ACKNOWLEDGMENTS

The author would like to thank Translational Chemical Biology Lab members for the use of their equipment during the synthesis and T. Adachi, Research Promotion Institute, Oita University, for the ESI-MS measurements. This work was supported by JSPS KAKENHI grant numbers JP16K13980, the Sumitomo Foundation, the Watanabe Foundation, and Iketani Science and Technology Foundation.

■ REFERENCES

(1) Simons, K.; Ikonen, E. Functional rafts in cell membranes. *Nature* **1997**, *387*, 569−572.
(2) Lingwood, D.; Simons, K. Lipid rafts as a membrane-organizing principle. *Science* **2010**, *327*, 46−50.
(3) Brown, D. A. Seeing is believing: Visualization of rafts in model membranes. *Proc. Natl. Acad. Sci. U.S.A.* **2001**, *98*, 10517−10518.
(4) Dietrich, C.; Bagatolli, L. A.; Volovyk, Z. N.; Thompson, N. L.; Levi, M.; Jacobson, K.; Gratton, E. Lipid rafts reconstituted in model membranes. *Biophys. J.* **2001**, *80*, 1417−1428.
(5) Veatch, S. L.; Soubias, O.; Keller, S. L.; Gawrisch, K. Critical fluctuations in domain-forming lipid mixtures. *Proc. Natl. Acad. Sci. U.S.A.* **2007**, *104*, 17650−17655.
(6) Davis, J. H.; Clair, J. J.; Juhasz, J. Phase equilibria in DOPC/DPPC-d62/cholesterol mixtures. *Biophys. J.* **2009**, *96*, 521−539.
(7) Stöckl, M.; Plazzo, A. P.; Korte, T.; Herrmann, A. Detection of lipid domains in model and cell membranes by fluorescence lifetime imaging microscopy of fluorescent lipid analogues. *J. Biol. Chem.* **2008**, *283*, 30828−30837.

(8) Juhasz, J.; Davis, J. H.; Sharom, F. J. Fluorescent probe partitioning in giant unilamellar vesicles of 'lipid raft' mixtures. *Biochem. J.* **2010**, *430*, 415−423.
(9) Juhasz, J.; Sharom, F. J.; Davis, J. H. Quantitative characterization of coexisting phases in DOPC/DPPC/cholesterol mixtures: comparing confocal fluorescence microscopy and deuterium nuclear magnetic resonance. *Biochim. Biophys. Acta* **2009**, *1788*, 2541−2552.
(10) Baumgart, T.; Hess, S. T.; Webb, W. W. Imaging coexisting fluid domains in biomembrane models coupling curvature and line tension. *Nature* **2003**, *425*, 821−824.
(11) Veatch, S. L.; Keller, S. L. Separation of liquid phases in giant vesicles of ternary mixtures of phospholipids and cholesterol. *Biophys. J.* **2003**, *85*, 3074−3083.
(12) Morales-Penningston, N. F.; Wu, J.; Farkas, E. R.; Goh, S. L.; Konyakhina, T. M.; Zheng, J. Y.; Webb, W. W.; Feigenson, G. W. GUV preparation and imaging: minimizing artifacts. *Biochim. Biophys. Acta* **2010**, *1798*, 1324−1332.
(13) Loew, M.; Springer, R.; Scolari, S.; Altenbrunn, F.; Seitz, O.; Liebscher, J.; Huster, D.; Herrmann, A.; Arbuzova, A. Lipid domain specific recruitment of lipophilic nucleic acids: a key for switchable functionalization of membranes. *J. Am. Chem. Soc.* **2010**, *132*, 16066−16072.
(14) Schade, M.; Knoll, A.; Vogel, A.; Seitz, O.; Liebscher, J.; Huster, D.; Herrmann, A.; Arbuzova, A. Remote control of lipophilic nucleic acids domain partitioning by DNA hybridization and enzymatic cleavage. *J. Am. Chem. Soc.* **2012**, *134*, 20490−20497.
(15) Yoshina-Ishii, C.; Miller, G. P.; Kraft, M. L.; Kool, E. T.; Boxer, S. G. General method for modification of liposomes for encoded assembly on supported bilayers. *J. Am. Chem. Soc.* **2005**, *127*, 1356−1357.
(16) Kurz, A.; Bunge, A.; Windeck, A. −K.; Rost, M.; Flasche, W.; Arbuzova, A.; Strohbach, D.; Müller, S.; Liebscher, J.; Huster, D.; Herrmann, A. Lipid-anchored oligonucleotides for stable double-helix formation in distinct membrane domains. *Angew. Chem., Int. Ed.* **2006**, *45*, 4440−4444.
(17) Chen, H.; Ahsan, S. S.; Santiago-Berrios, M. B.; Abruña, H. D.; Webb, W. W. Mechanisms of quenching of Alexa fluorophores by natural amino acids. *J. Am. Chem. Soc.* **2010**, *132*, 7244−7245.
(18) MacKenzie, R. E.; Foery, W.; McCormick, D. B. Flavinyl Peptide. II. Intramolecular interactions in flavinyl aromatic amino acid peptides. *Biochem* **1969**, *8*, 1839−1844.
(19) García-Mouton, C.; Parra-Ortiz, E.; Malmsten, M.; Cruz, A.; Pérez-Gil, J. Pulmonary surfactant and drug delivery: Vehiculization of a tryptophan-tagged antimicrobial peptide over the air-liquid interfacial highway. *Eur. J. Pharm. Biopharm.* **2022**, *180*, 33−47.
(20) Oka, Y.; Miura, T.; Ikoma, T. Photogenerated radical pair between flavin and a tryptophan-containing transmembrane-type peptide in a large unilamellar vesicle. *J. Phys. Chem. B* **2021**, *125*, 4057−4066.
(21) Oka, Y.; Shishino, H. Fluorescence quenching of alexa fluor 488-labeled DNA by complementary Trp-containing PNA partitioned in liquid-ordered domains. *Chem. Lett.* **2017**, *46*, 1672−1675.
(22) Oka, Y.; Shishino, H. Fluorescence imaging of disrupted interfaces between liquid-ordered and liquid-disordered domains by a flavin-labeled PNA duplex. *ACS Omega* **2017**, *2*, 2912−2915.
(23) Jenssen, H.; Hamill, P.; Hancock, R. E. Peptide antimicrobial agents. *Clin. Microbiol. Rev.* **2006**, *19*, 491−511.
(24) van der Weerden, N. L.; Bleackley, M. R.; Anderson, M. A. Properties and mechanisms of action of naturally occurring antifungal peptides. *Cell. Mol. Life Sci.* **2013**, *70*, 3545−3570.
(25) Sun, S.; Zhao, G.; Huang, Y.; Cai, M.; Shan, Y.; Wang, H.; Chen, Y. Specificity and mechanism of action of alpha-helical membrane-active peptides interacting with model and biological membranes by single-molecule force spectroscopy. *Sci. Rep.* **2016**, *6*, 29145.
(26) Last, N. B.; Schlamadinger, D. E.; Miranker, A. D. A common landscape for membrane-active peptides. *Protein Sci.* **2013**, *22*, 870−882.
(27) Rakowska, P. D.; Jiang, H.; Ray, S.; Pyne, A.; Lamarre, B.; Carr, M.; Judge, P. J.; Ravi, J.; M. Gerling, U. I. M.; Koksch, B.; Martyna, G. J.; Hoogenboom, B. W.; Watts, A.; Crain, J.; Grovenor, C. R. M.; Ryadnov, M. G. Nanoscale imaging reveals laterally expanding antimicrobial pores in lipid bilayers. *Proc. Natl. Acad. Sci. U.S.A.* **2013**, *110*, 8918−8923.
(28) van Meer, G.; Voelker, D. R.; Feigenson, G. W. Membrane lipids: where they are and how they behave. *Nat. Rev. Mol. Cell Biol.* **2008**, *9*, 112−124.
(29) Sani, M.-A.; Separovic, F. How membrane-active peptides get into lipid membranes. *Acc. Chem. Res.* **2016**, *49*, 1130−1138.
(30) Deo, S.; Turton, K. L.; Kainth, T.; Kumar, A.; Wieden, H.-J. Strategies for improving antimicrobial peptide production. *Biotechnol. Adv.* **2022**, *59*, 107968 and the references cited in the paper.
(31) Gosse, C.; Boutorine, A.; Aujard, I.; Chami, M.; Kononov, A.; Cogné-Laage, E.; Allemand, J.-F.; Li, J.; Jullien, L. Micelles of lipid-oligonucleotide conjugates: Implications for membrane anchoring and base pairing. *J. Phys. Chem. B* **2004**, *108*, 6485−6497.
(32) Ugarte-Uribe, B.; Grijalvo, S.; Busto, J. V.; Martín, C.; Eritja, R.; Goñi, F. M.; Alkorta, I. Double-tailed lipid modification as a promising candidate for oligonucleotide delivery in mammalian cells. *Biochim. Biophys. Acta* **2013**, *1830*, 4872−4884.
(33) Chakrabarti, M. C.; Schwarz, F. P. Thermal stability of PNA/DNA and DNA/DNA duplexes by differential scanning calorimetry. *Nucleic Acids Res.* **1999**, *27*, 4801−4806.
(34) Frier, C.; Décout, J.-L.; Fontecave, M. Method for preparing new flavin derivatives: Synthesis of flavin-thymine nucleotides and flavin-oligonucleotide adducts. *J. Org. Chem.* **1997**, *62*, 3520−3528.
(35) Ikeda, H.; Yoshida, K.; Ozeki, M.; Saito, I. Synthesis and characterization of flavin-tethered peptide nucleic acid. *Tetrahedron Lett.* **2001**, *42*, 2529−2531.

https://doi.org/10.1021/acsomega.2c06463
ACS Omega 2023, 8, 1109−1113